# Effects of PODE/diesel blends on particulate matter emission and particle oxidation characteristics of a common-rail diesel engine

Junheng Liu[a]*, Zengguang Liu[a], Lejian Wang[a], Pan Wang[a], Ping Sun[a], Hongjie Ma[b], Pengcheng Wu[a]

[a] School of Automotive and Traffic Engineering, Jiangsu University, Zhenjiang 212013, China

[b] Institute of Industrial Research, University of Portsmouth, Portsmouth, Hampshire PO1 2EG, United Kingdom

* Corresponding author at: Jiangsu University, 301 Xuefu Road, Zhenjiang, Jiangsu 212013, China.

Email address: liujunheng365@163.com

Abstract: The current study focused on the particulate matter emissions of polyoxymethylene dimethyl ethers (PODE)/diesel blends with PODE blending ratios of 0, 10%, 20% and 30% have been experimentally investigated in a common-rail engine. The influences of PODE blending ratio on the smoke emission, particle size distribution and particle oxidation characteristic are discussed. Results show that the addition of PODE in diesel fuel can effectively reduce smoke emission and its decreasing range becomes larger with increasing PODE blending ratio. With the increment in PODE blending ratio, the particle concentration distribution moves towards the direction of small particle size, and the total particle number concentrations decrease. Besides, the peak values of particle number concentration, surface area concentration, and volume concentration are all decreased. Adding PODE in diesel fuel increases the soluble organic fraction (SOF) content of particles, rises maximum weight loss rate of particles, and lower the peak temperature of particles. Also, the activation energy of pyrolysis reaction of particles decreases, which indicates that the oxidation of particles becomes easier as PODE blending ratio increases. The apparent morphology of particles was measured by scanning electron microscope, and the results show that the morphology of particles sample are mostly chain like or flocculent.

Keywords: Diesel engine; Polyoxymethylene dimethyl ethers; Particulate matter emission; Particle oxidation; Particle number

## 1. Introduction

The diesel engines, due to their higher power performance, efficiency and durability, have been widely employed in power generation and transportation for more than one hundred years. The increasing thermal efficiency and simultaneously reducing emissions for diesel engines are the primary objectives owing to fossil fuel shortage and environmental pollutions [1-3]. Particulate matter (PM) is the most prominent emission pollutant from diesel engines. In recent years, the total mass of PM emissions has been greatly reduced by various advanced combustion concepts and after-treatment technologies. Moreover, the focus of PM emission becomes the exhaust gas particle number concentration and size distribution. Diesel engine exhaust particle size distribution divided by nucleation-mode particles (diameter of the particle, 5 nm<$D_p$<50 nm), accumulation-mode particles (50 nm<$D_p$<1000 nm) and coarse-mode particles ($D_p$>1000 nm) [4,5]. Nucleation-mode particles are constituted by that particulate core, formed by solid carbon particles combined with sulfuric acid vapor solid converted by part of the sulfur in diesel, adsorbs volatile organic compounds during the in-cylinder combustion process. Accumulation-mode particles are composed of nucleation-mode particles that are further aggregated into agglomerates and coagulated with semi-volatile substances such as sulfuric acid and HC [6].

Several studies confirmed that oxygenated fuel, playing an oxygen self-supplying role in the combustion process, can effectively reduce soot and particle emissions [7-10]. Polyoxymethylene dimethyl ethers (PODE) with no C-C bond, is a promising novel fuel for PM emissions decreased due to the low viscosities and pour points, low distillation temperatures, high oxygen contents and high cetane numbers [11,12]. The production costs of PODE are lower than that of hydrocarbons, especially in China, where the coal-based $C_1$ compounds like methanol and formaldehyde are oversupplied and low-cost commercial production of PODE has been realized [13,14]. There has been a great deal of studies related to combustion performance and emissions of diesel engine with PODE [15,16]. Pellegrini et al. [17] investigated the effects of blending

7.5% PODE into diesel on the emissions in a three cylinder, four-stroke direct injection (DI) Euro III light-duty diesel engine. Their results indicated that the smoke and PM emissions were reduced by 32% and 13%, but the polycyclic aromatic hydrocarbon (PAH) emissions and particles ($D_p$<30nm) marginally increased. Liu et al. [18] studied the effect of the addition of 15% and 25% PODE (in volume) on performance and exhaust emissions in a four-cylinder, turbocharged, heavy-duty, DI diesel engine. Their results showed that the NOx-soot trade-off relationship can be dramatically improved by fueling diesel/PODE blends. The weighted results over the World Harmonized Stationary Cycle (WHSC) indicated that the raw soot emission of blending 25% PODE into diesel can meet the Euro VI soot emission standard when the weighted NOx is controlled at 2.7 g/(kW·h).

Particle emissions represent a critical issue in particular for diesel engines blended with PODE, because of their effect on human health. In order to make it clear of the source of PM emitted from a diesel engine blended with PODE, lots of studies have explored the influences of PODE on particles [19,20]. Barro et al. [21] investigated the performance of a research single cylinder heavy-duty 4-stroke diesel engine fueled with PODE/diesel blends (20% and 80% PODE in volume) and found that the particle emissions using PODE showed high number concentration (compared with pure diesel) in a size range mainly below 20 nm. Their results reported that there was a bimodal distribution in the particle emission of PODE/diesel fuel. Moreover, the peak value of small particle size increased and the peak value of large particle size decreased with the proportion of PODE increasing. Recent evidence [22,23] indicates that PODE can be blended with diesel in various ratios and direct application of PODE can reduce soot and PM emissions without changing the existing diesel engine structure. Nevertheless, previous studies paid little attention on the effects of PODE blending ratio on particle size distribution and particle oxidation characteristics in diesel engine, and further investigation about them is necessary. Moreover, there are no enough research about the microstructures for particles of blending PODE. From this view points of particles reduction, it is necessary to carry out the

research on the microstructures for particles.

In current study, the exhaust PM emissions of pure diesel and PODE/diesel blends were systematically explored on a 4-cylinder turbocharged intercooled common-rail diesel engine. Firstly, the effects of PODE blending ratios on the exhaust particle number concentration, surface area concentration, and volume concentration were discussed with a particle size spectrometer. Secondly, the oxidation characteristics of particles were studied by thermogravimetric analysis (TGA), and particle activation energy was calculated using the Coast-Redfern integral method. Finally, the microstructures of exhaust particles and smoke emissions were analyzed using scanning electron microscopy and smoke meter, respectively.

## 2. Experimental setup and procedure

### 2.1. Experimental apparatus

The experimental engine employed for the current study was a four cylinder, four-stroke, turbocharged, intercooled, common-rail diesel engine. Fig. 1 shows schematic diagram of the experimental setup. The diesel engine structure and control strategy remain unchanged, and the main engine specifications are listed in Table 1. In the experiment, the engine was controlled by an electrical dynamometer (AVL 504/4.6 SL) coupled with an auto-testing and control system (AVL PUMA OPEN), which adjusts the torque output and keeps the speed constant. The instantaneous blended fuel consumption rate was measured using an intelligent fuel consumption meter (AVL 735s). The smoke emission was measured using a filter-type smoke meter (AVL 415s), which detects soot particles in diesel engine exhaust through the blackness of filter paper [24]. The particle size distribution and the number of that were measured using an engine exhaust particle size spectrometer (TSI EEPS-3090), which can measure particle size from 5.6 nm to 560 nm [25]. EEPS-3090 used a dilution sampling scheme to measure particle concentration. The dilution ratio of the first stage dilution system was set to 100:1, and the secondary dilution ratio was set to 2:1, thus the total dilution ratio was 200:1. Moreover, the EEPS, the heating temperature of the dilution system controlled to 120°C,

can detect a complete particle size distribution map within 0.1s and output the number of particles and particle size distribution of 32 channels simultaneously. During the testing, 100s was taken as a time period to calculate the average distribution map of particle size. The particle samples were collected using a particle grading sampling device (MSP MOUDI-100). The engine exhaust, diluted and cooled, was sampled at 30 L/min for 30 minutes under the action of a vacuum pump and collected PM for analysis via Φ47 aluminum foil filter paper. The oxidation properties of PM samples with different test fuels were measured using a synchronous thermal analyzer (METTLER TGA110) [26].

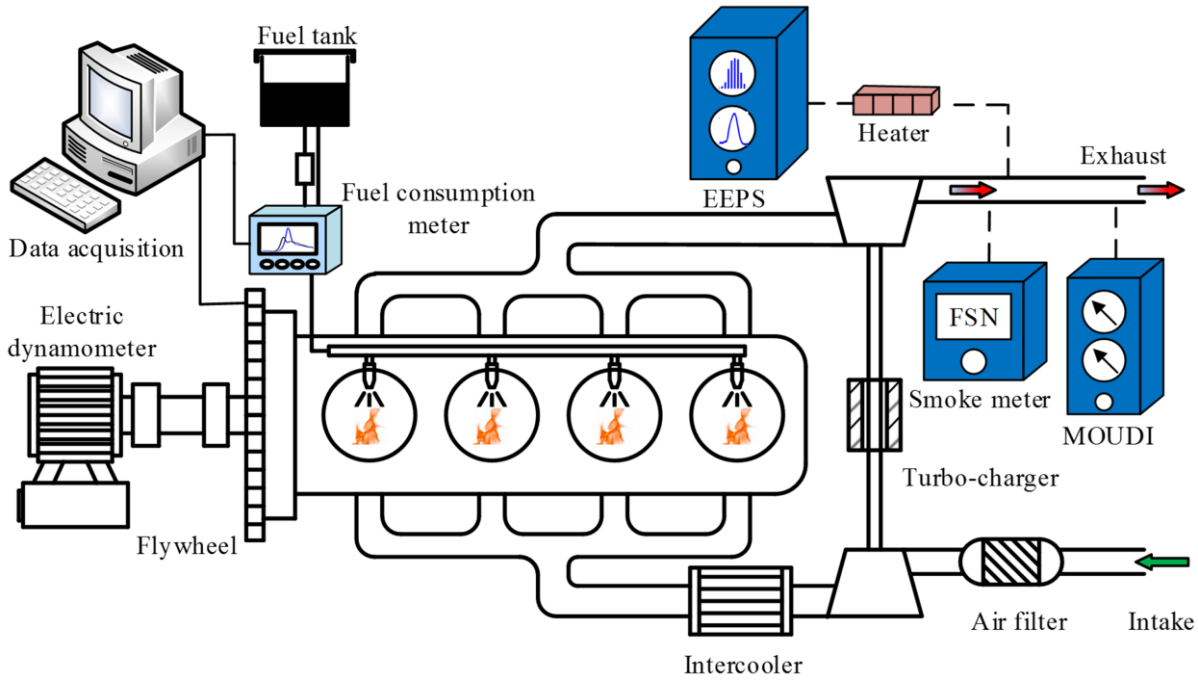


**Fig.1.** Schematic diagram of the experimental setup.

**Table 1** Specifications of experimental engine.

| Item | Specification |
|---|---|
| Engine type | In-line, 4 cylinder, 4 valves, turbocharged, water cooler |
| Bore × Stroke | 108 mm × 118 mm |
| Displacement | 4.32 L |
| Compression ratio | 17.5 : 1 |
| Rated power | 98 kW (2400 r/min) |
| Maximum torque | 400 N·m (1400~1600 r/min) |
| Combustion chamber shape | Direct injection ω type |
| Fuel injection system | Electronically controlled common-rail |

## 2.2. Test fuels

The basic fuels adopted in the test were commercial ultra-low sulfur Euro VI diesel and PODE. Diesel fuel was produced by Sinopec Group, whose sulfur content is less than 5 ppm. Diesel is composed of numerous $C_9$-$C_{21}$ hydrocarbon species including paraffins, olefins, cycloparaffins and aromatics, and they are mainly n-paraffins, isoparaffins, naphthencs, aromatics and heteratomics [27]. PODE fuel was synthesized and separated by Qingdao Tongchuan Company, whose purity is 99%. PODE is a kind of acetal polymer with chain of the molecule of (-O-$CH_2$-) as the main chain, and its molecular formula is $CH_3O(CH_2O)_nCH_3$, where n stands for the polymerization degree and n≥1 [28]. $PODE_3$, $PODE_4$, $PODE_5$ and $PODE_6$ represent PODE fuels with polymerization degrees of 3, 4, 5 and 6, and their mass fractions are 39.3%, 25.1%, 21.3% and 14.3%, respectively in the test fuel of PODE. PODE was blended with diesel fuel at volume blending ratios of 0%, 10%, 20% and 30% to prepare PODE/diesel blends at room temperature and atmospheric pressure, and marked as D, P10, P20 and P30 fuels, respectively. The physical and chemical properties of the test fuels are given in Table 2. With the increment of PODE blending ratio, the cetane number, oxygen content and latent heat of vaporization for blend fuels increase, while the low heating value gradually decreases [29].

**Table 2** Physicochemical properties of diesel, PODE and blended fuel.

| Item | D | PODE | P10 | P20 | P30 |
|---|---|---|---|---|---|
| Density at 15 °C (kg/m$^3$) | 822 | 1050 | 845 | 868 | 890 |
| Proportion of O (%) | 0 | 42.7 | 5.9 | 11.4 | 16.7 |
| Proportion of C (%) | 86.5 | 44.1 | 81.2 | 76.2 | 71.4 |
| Proportion of H (%) | 13.49 | 8.78 | 12.9 | 12.4 | 11.82 |
| Sulfur content (ppm) | 5.0 | 0 | 4.4 | 3.8 | 3.2 |
| Lower heating value (MJ/kg) | 42.6 | 17.8 | 39.6 | 36.7 | 33.9 |
| Cetane number | 51.5 | 76 | 54 | 56.4 | 58.9 |
| Latent heat of vaporization (kJ/kg) | 250 | 359 | 263 | 277 | 289 |
| End of boiling point (°C) | 310 | 180 | - | - | - |
| Kinematic viscosity at 20 °C (mm$^2$/s) | 4.8 | 1.05 | 4.43 | 4.05 | 3.68 |

## 2.3. Test conditions and procedure

In the experiment, the effects of PODE/diesel blends (D, P10, P20 and P30) on PM emissions were analyzed under the engine loads of 0%, 25%, 50%, 75% and 100% at rated speed of 2400 r/min. Ambarish

et al. also selected the rated condition as the test condition in the exploration of combustion and emission characteristics of diesel engine with alcohol addition [30]. Firstly, the smoke emission of four test fuels versus engine loads was measured using the smoke meter, and the total particle number concentration was analyzed using the engine exhaust particle size spectrometer correspondingly. Meantime, the effects of PODE blending ratio on the particle diameter, particle surface area and particle volume distributions of 25% and 100% loads were analyzed based on the measurement results. Finally, the PM samples of different test fuels under rated condition for thermogravimetric testing and micro-morphology analysis were collected using the particle grading sampling device [31]. The TGA of particle sample was conducted on a thermogravimetric analyzer, which had built-in high precision electronic balance and temperature sensor. The thermal weight loss process was recorded on-line by the data recording system. In each test, particle sample with about 3mg was heated in the temperature range of 20~800°C, and the heating rates was set to 15°C/min. High purity $N_2$ and the air were taken as the protective gas and the reaction air, respectively, and their flow rates were both set to a constant value of 50 mL/min. Thermogravimetric (TG) curves were obtained by continually recording the mass loss with increasing temperature, and the derivative thermogravimetric (DTG) curves were obtained by differentiating TG curves. The steady-state tests were repeated at least twice to ensure that the results are repeatable within the experimental uncertainty. The oxidation property of PM was obtained from the TG curve and the DTG curve, and their pyrolysis kinetic parameters were calculated by the Coast-Redfern integral method. After surface gold spray treatment, the microstructures of particle samples with four testing fuels were observed by a thermal field emission scanning electron microscopy (SEM) (HITACHI S-4800). The resolutions of S-4800 were 1.0 nm (15 kV) and 2.0 nm (1 kV), and its amplification range was $20\sim8\times10^5$ times.

To improve measurement accuracy, experimentation with each test fuel was carried out three times and their average values were considered for further calculation. During the testing process, there were several

chances for errors and uncertainties due to calibration, observation, instrument selection, working condition, environmental condition, etc. In order to prove the level of accuracy in measured and calculated readings, uncertainty analysis must be performed. Also, for normalizing the fixed/random errors occurred due to manufacturing syntax of various equipment, uncertainties were estimated in measured parameters using analytical method and the calculated uncertainties for various measured quantities were listed in Table 3.

**Table 3** Accuracy and uncertainty of measured parameters.

| Instrument | Measured parameters | Range | Accuracy | Uncertainty (%) |
|---|---|---|---|---|
| Electric dynamometer | Speed | 0~5000r/min | 0.04% | - |
| | Torque | 0~700N·m | 0.4% | - |
| Fuel consumption meter | Fuel consumption | 0~125kg/h | 0.12% | 0.5 |
| Smoke meter | Smoke | 0~10FSN | 0.001FSN | 0.5 |
| Thermal analyze | Weight loss rate | 0~10 mg | 0.1μg | 2.0 |
| Engine Exhaust Particle Sizer | Particle size | 5.6~560nm | 0.1nm | - |
| MOUDI-100 | Particle sampling | 0.18~18μm | 1nm | 0.2 |

# 3. Results and discussion

## 3.1. Smoke emission

Fig. 2 reveals the effect of PODE blending ratio on smoke emission under different engine loads of 2400r/min. It can be observed from Fig. 2 that the addition of PODE into diesel fuel can effectively decrease the smoke emission, and the reduction obviously rises with the increase of PODE blending ratio and engine load. Compared with pure diesel, the smoke emission levels of P10, P20 and P30 are decreased by 29.7%, 67.8% and 82.4% at rated condition. Generally, in-cylinder soot formation of diesel engine is due to the local hypoxia and high-temperature fuel cracking caused by the uneven mixture of fuel and gas, which is mainly generated in the diffusion combustion stage. Because of the low viscosity and boiling point of PODE fuel, adding PODE in diesel fuel is conducive to the atomization and evaporation of the blended fuel, and also can improve the uniformity of fuel-gas mixture [32,33]. The addition of PODE will increase oxygen content of the blends, which plays a self-oxygen supply role during combustion, thus improving diffusion combustion, and promoting the post oxidation process of carbon smoke in the subsequent expansion and

exhaust stages. The results of chemical reaction kinetics calculation show that carbon atoms existing as C-O bonds in PODE are difficult to participate in the free radical reactions of small-molecule formation. Thus, the substitution of PODE for diesel reduces the generation amount of soot precursor PAH [29,34]. Moreover, a large number of OH oxidation groups are formed in the early stage of PODE combustion, which can directly react with ethylene or acetylene, thereby inhibiting the formation of PAH and the growth of soot rings [35]. The above reasons lead to the reduction of exhaust smoke with the addition of PODE in diesel fuel.

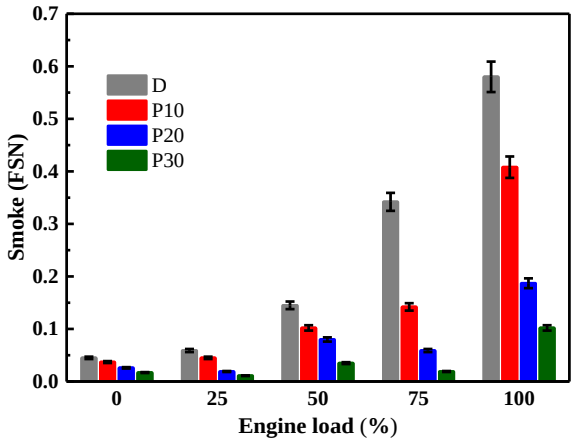


**Fig. 2.** Effects of PODE blending ratio on smoke emission for various loads.

### 3.2. Exhaust particle number and particle size distribution

In general, PAH adsorbed on the surface of carbon particles will damage human health. In terms of harmfulness to human body and atmospheric environment, the quality of particle emission does not play a decisive role, but the size distribution and number concentration of particles are more important. China VI emission regulations for diesel vehicles clearly defines the emission limits of total particle number, which have been carried out since 2019.

Fig. 3 presents the effect of PODE blending ratio on total particle number concentration under different engine loads of 2400r/min. It can be observed that total particle number concentration of the blends rises with increasing engine load whereas decreases with increasing PODE blending ratio, and diesel fuel is the largest producer of total particle number in all conditions. Under rated condition, the total number of exhaust

particles with P10, P20 and P30 fuels are decreased by 15.5%, 27.0% and 28.1% as compared with pure diesel, respectively. This is mainly due to the higher cetane number, lower sulfur and aromatics contents, and lower viscosity of PODE comparing to diesel fuel. With the addition of PODE in diesel fuel, the blends have higher cetane number and oxygen content, and the ignition timing is advanced and the burning speed improves rapidly [36], which helps to reduce particle emission. Because of the high carbon content and stable chemical structure of aromatics, it is easy to form soot particles during combustion. The blended fuel has less aromatics, so adding PODE to diesel fuel can reduce the exhaust particles of accumulation-mode for diesel engines [37]. The sulfur in the fuel will be discharged in the form of sulfate particles after combustion stage, thus the lower sulfur content of the blended fuel will help to reduce the sulfated particles of nucleation-mode [38,39]. The lower viscosity and boiling point of the blends can improve the interior fuel atomization inside the cylinder, which makes combustion of air-fuel mixture more sufficient, resulting in the reduction of the formation of nucleation-mode particles. All of these factors together make the total particle number emission decrease with the addition of PODE in diesel fuel.

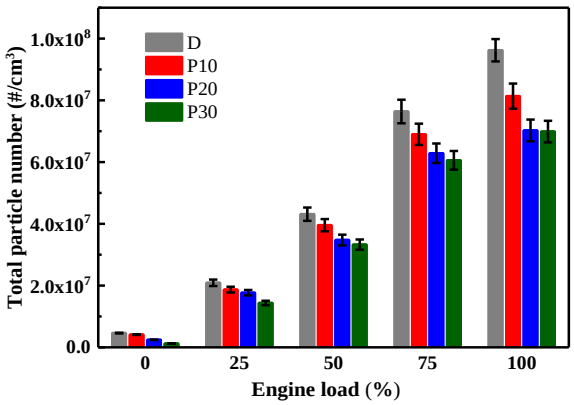


**Fig. 3.** Effects of PODE blending ratio on total particle number concentration for various loads.

Fig. 4 illustrates the effect of PODE blending ratio on particle number concentration distribution of the blends at 25% and 100% loads of 2400 r/min. It can be seen from Fig. 4(a) that at 25% engine load, the particle number concentration with particle size distribution appears a bimodal curve: the first peak occurs at 10~20 nm, belonging to the nucleation-mode scope; the second obvious peak occurs at 50~70 nm, belonging

to the accumulation-mode scope. With the increment in PODE blending ratio, the peak concentration of accumulation-mode particles gradually decreases and the peak concentration of nucleation-mode particles gradually increases, while the whole distribution curve of particle number concentration moves to the direction of small particle size. As seen in Fig. 4(b), the particle number concentration distribution acts as a single peak presenting in the range of 30~40 nm under rated condition. The particle emission of the blends is mainly in the nucleation-mode region, and the number concentration of accumulation-mode particles is relatively low, besides the peak concentration of exhaust particles drops down with an increase in PODE blending ratio. Nucleation-mode particles are usually the primary carbon particles formed by nonuniform combustion in cylinder and the secondary particles formed by dilution and cooling nucleation of precursors such as HC and sulfuric acid, etc. And nucleating effect is affected by the specific surface area of particles, ambient humidity and temperature in the exhaust [40]. The concentration of accumulation-mode particles with large particle size decreases significantly with the addition of PODE into diesel fuel, which reduces the adsorption capacity of gaseous precursors (HC or sulfuric acid) on the surface of accumulation-mode particles and increases the nucleating effect during the exhaust and dilution processes, resulting in an increase of the number concentration of nucleation-mode particles.

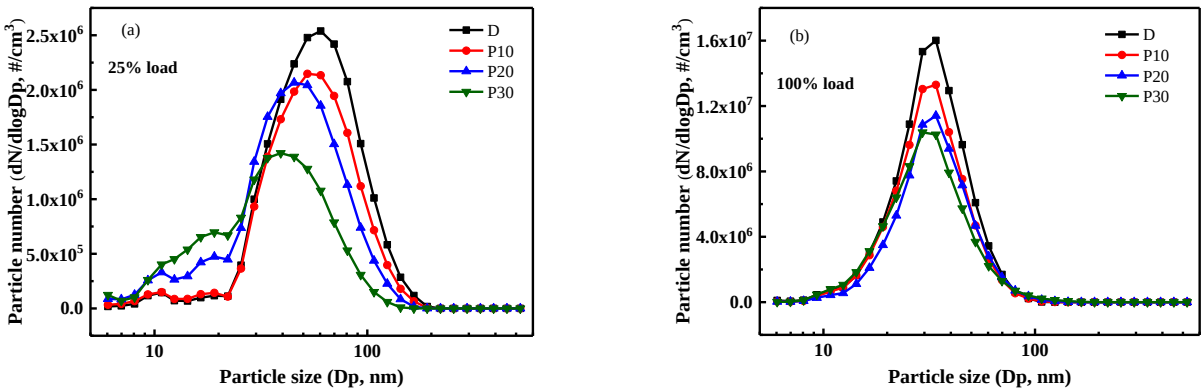


**Fig. 4.** Effects of PODE blending ratio on particle number concentration distribution: (a) 25% load; (b) 100% load.

Fig. 5 shows the proportion of particle size distribution from diesel exhaust versus PODE blending ratios, which is obtained by summing the particle number concentration in different particle size segments in Fig. 4.

With the increase of PODE blending ratio, the proportion of ultra-fine particles ($D_p$<22 nm) increases significantly, and the proportion of nucleation-mode particles increases correspondingly, while the proportion of accumulation-mode particles decreases gradually, especially at low load. At 25% load, the proportions of nucleation-mode particles for pure diesel, P10, P20 and P30 fuels are 37.6%, 41.7%, 57.0% and 70.8%, and the corresponding proportions of accumulation-mode particles are 62.4%, 58.3%, 43.0% and 29.2% respectively. The reason for the increase in the number of nucleation-mode particles and the decrease in the number of accumulation-mode particles is that the blends have larger penetration distance, good evaporation and atomization characteristics [41,42]. The fuel concentration in the injection periphery and near-wall region is too lean to burn completely, which increases the generation of SOF, thus leading to the increase of nucleation-mode particles. The smoke emission of the blends is lower, and the adsorption capacity of the accumulation-mode particles for SOF is reduced, further leading to the increase of nucleation-mode particles [43]. Due to the self-contained oxygen of the blends, some accumulation-mode particles will be oxidized to nucleation-mode particles in post-combustion period [44], which reduces the proportion of accumulation-mode particles.

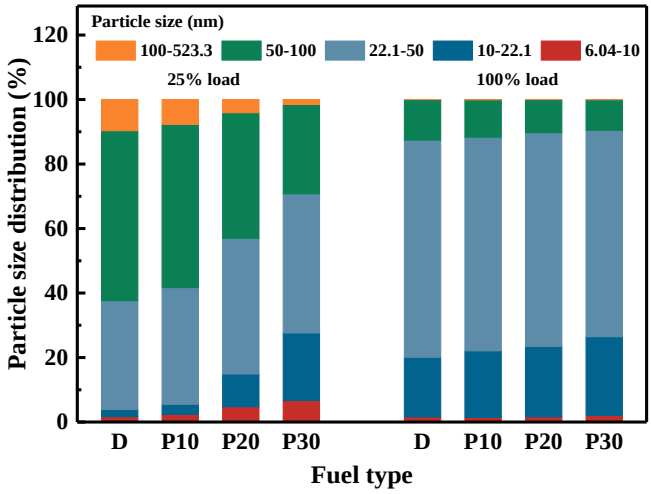


**Fig. 5.** Effects of PODE blending ratio on particle size contribution at 25% and 100% loads.

The larger the surface area of the particles is, the stronger the absorption capacity of organic components with high boiling point in exhaust gas is, the greater the toxicity is, the more likely it is to cause harm to

human body. Fig. 6 presents the effect of PODE blending ratio on particle surface area concentration distribution of the blends at 25% and 100% loads of 2400 r/min. As shown in Fig. 6(a), the varying curve of particle surface area concentration acts as a single peak morphology, mainly distributed in the accumulation-mode state, and the peak appears at about 80 nm. With the increase of PODE blending ratio, the peak value of particle surface area concentration decreases obviously, and the peak position gradually shifts to the left. This shows that adding PODE to diesel fuel can significantly reduce the emission of accumulation-mode particles, which is consistent with the results in Fig. 4(a), and the shift of peak position to the left indicates that the proportion of ultrafine particles increases, which is consistent with the results in Fig. 5. The change trend presented in Fig. 6(b) is similar to that of Fig. 6(a), but it is mainly distributed in the nucleation-mode state. The peak appears at about 40 nm, and the overall peak value of 100% load is higher than that of 25% load. It is mainly due to the high combustion temperature and exhaust temperature at high load, which makes the accumulation-mode particles oxidize to form nucleation-mode particles, so that both the peak value of particle number concentration and the proportion of ultra-fine particles become larger [4, 45], which are identical with the results presented in Fig. 4.

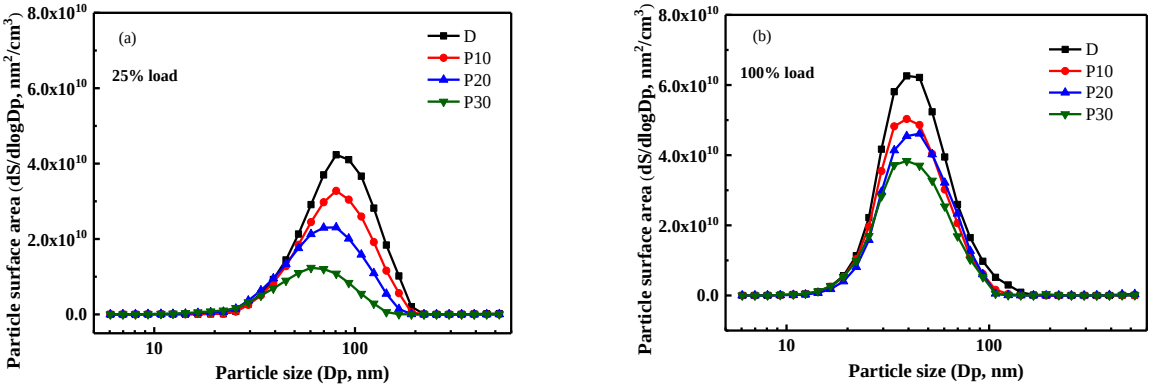


**Fig. 6.** Effects of PODE blending ratio on particle surface area concentration distribution: (a) 25% load; (b) 100% load.

Fig. 7 reveals the effect of PODE blending ratio on particle volume concentration distribution of the blends at 25% and 100% loads of 2400 r/min. It can be seen that the particle volume concentration decreases with the increase of PODE blending ratio, and its distribution presents a single peak. The peak position of

particle volume concentration moves to large particle size compared with the peaks of particle number and particle surface area concentrations. Particle volume concentration peaks of 25% and 100% loads appear at 100nm and 50nm respectively, and particle volume concentration of 100% load is lower than that of 25% load. This is because a small number of accumulation-mode particles will inhibit the adsorption and coagulation of nucleation-mode particles, resulting in an increase of nucleation-mode particles with engine load, and the influence of small particles on particle volume concentration distribution is so little [46,47]. The results also show that the addition of PODE in diesel fuel can reduce particle volume concentration, which makes it easier for diesel exhaust particles to sink and shortens the residence time in the air.

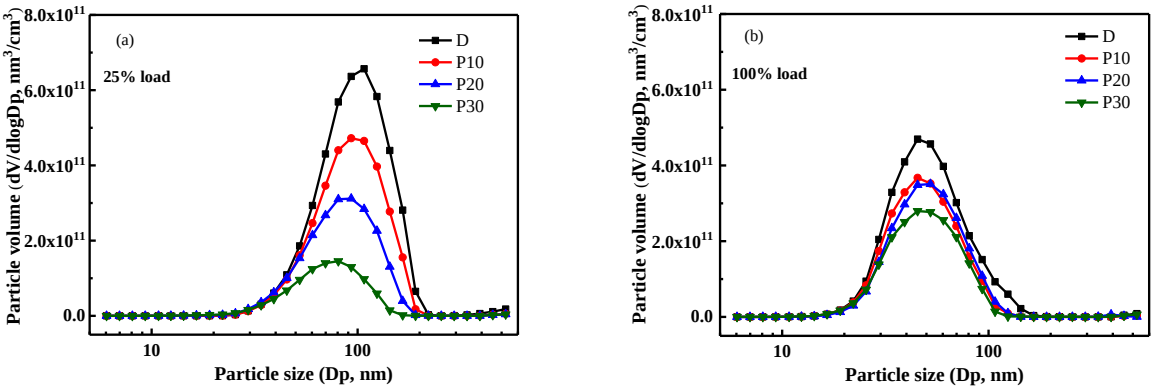


**Fig. 7.** Effects of PODE blending ratio on particle volume concentration distribution: (a) 25% load; (b) 100% load.

### 3.3. Particle oxidation property

Fig. 8 illustrates the particle TG and DTG curves of the blends with different PODE blending ratios at rated condition and in air atmosphere. It can be observed from Fig. 8(a) that the heating process of particles is mainly divided into three reaction stages: the first stage is the water evaporation stage (40~110 °C); the second stage is the SOF volatilization and oxidation (120~250 °C); the third stage is the particles oxidation (400~650 °C). As shown in Fig. 8(b), the weight loss rate increases significantly when the TGA temperature is higher than 120 °C, which is the oxidation and volatilization of high volatile SOF. However, as the TGA temperature reaches 200 °C, the weight loss rate gradually decreases, which is the oxidation and volatilization of low volatile SOF. There are two obvious peaks of weight loss rate in the DTG curve. The

first peak of weight loss rate appears at about 160 °C, which indicates the pyrolysis process of SOF components in the air atmosphere. The heat volatilization of SOF is accompanied by the oxidation reaction under the action of $O_2$, which makes the weight loss rate of particles increase significantly. The second peak of weight loss rate appears near 580 °C, which indicates the mass change process of soot oxidation. The data show that soot components in the particles of diesel, P10, P20 and P30 fuels account for 88.1%, 85.8%, 84.2% and 83.6%, and SOF components account for 8.7%, 11.6%, 12.9% and 13.6%, respectively. The peak values of absolute weight loss rate are 0.41, 0.46, 0.48 and 0.52 %/°C, and the corresponding temperatures of the peaks are 584, 580, 576 and 569 °C, respectively. It can be seen that with the increase of PODE blending ratio, the mass fraction of SOF component increases, the mass fraction of soot component decreases, the weight loss rate increases, and the peak temperature decreases. This is mainly due to the increment in the oxygen content of the blends with addition of PODE, more oxygen-containing groups will be adsorbed on the surface of particles after combustion, so the oxidation combustion rate of SOF component becomes faster. Fuel self-contained oxygen also improved the oxygen deficient condition of combustion in the cylinder. The amount of OH radicals generated in the initial combustion stage increase [48], and the oxidation of OH reduces PAH and its precursor, inhibiting the growth of soot particles, thus the emission of soot particles is less and the particle size is small. After adding PODE, the C-H bond far away from oxygen-containing group in soot particles breaks first to form more organic carbon, which has stronger oxidation characteristics than element carbon. As a result, once the temperature rises to a certain value, the organic carbon will be oxidized and burned rapidly, resulting in an increase in the decline rate of soot mass [49,50].

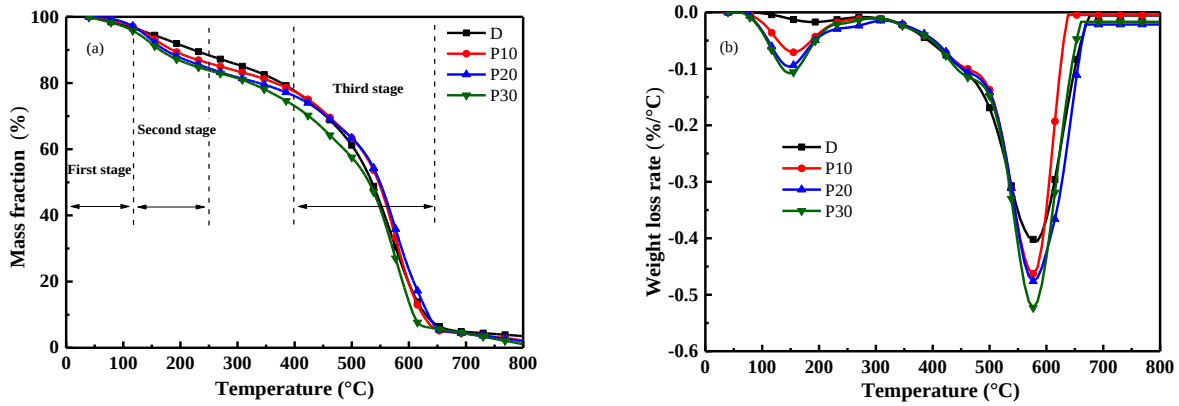


**Fig. 8.** TG and DTG curves of particle samples for various PODE blending ratios: (a) TG curve; (b) DTG curve.

Pyrolysis kinetics analysis of particle samples with the blends was carried out in the air atmosphere with Coats-Redfern method to obtain the reaction activation energy parameters of particles, which can be used to judge the difficulty of particle oxidation with different PODE blending ratios. Generally, activation energy refers to the minimum energy required for molecules to change from normal state to active state in chemical reactions, and the higher the activation energy is, the more energy is needed for pyrolysis. The equation for calculating the pyrolysis reaction of diesel exhaust particles by Coast-Redfern method is as follows:

$$G(\alpha)=\int_0^{\alpha}\frac{1}{(1-\alpha)^n}d\alpha=\int_0^{T}\frac{A}{\beta}\mathrm{e}^{-\frac{E}{RT}}dT \tag{1}$$

where $\alpha$ denotes the conversion rate of particle sample (%); $A$ denotes the pre-exponential factor ($min^{-1}$); $T$ denotes the reaction temperature (K); $E$ denotes activation energy (kJ/mol); $R$ denotes the ideal gas constant (8.314J/(K·mol)); $\beta$ denotes the heating rate (K/min), and is set to 15 K/min in the experiment; $n$ denotes the reaction order, and is often taken as 1 in the oxidation environment for diesel particles.

Sort out and simplify Eq. (1) to get Eq. (2):

$$\ln\left[\frac{-\ln(1-\alpha)}{T^2}\right]=\ln\left(\frac{AR}{\beta E}\right)-\frac{E}{RT} \tag{2}$$

Eq. (2) be regarded as one-variable linear equation with a slope of $-\frac{E}{R}$, an independent variable of $\frac{1}{T}$ and a dependent variable of $\ln\left[\frac{-\ln(1-\alpha)}{T^2}\right]$, and then $E$ and $A$ are can be calculated from the fitting straight line. Fig. 9 presents the pyrolysis characteristic curves of particle samples with four test fuels obtained using

fitting method, while the corresponding fitting equations and kinetic parameters of soot particles in the most intense reaction stage are listed in Table 4. Calculation results show that the fitting linear coefficients of all curves are greater than 0.95, which indicates that the ideal degree of fitting. The activation energy of particle pyrolysis reaction decreases with the addition of PODE in diesel fuel, and it decreases from 47.4 kJ/mol to 43.2 kJ/mol as PODE blending ratio increases from 0 to 30%. The result is consistent with the trends that the weight loss rate of soot particles rises and the peak temperature reduces with blending PODE in Fig. 8(b). This is due to the increase of organic carbon content in soot particles under the action of oxygen-containing group after adding PODE to diesel fuel. In addition, the disorder degree of soot particles increases and the graphitization degree decreases with an increase in the proportion of ultrafine particles for the blends, which makes the particles easier to be oxidized. Therefore, the energy required in the particle pyrolysis process decreases, and the reaction activation energy decreases [51].

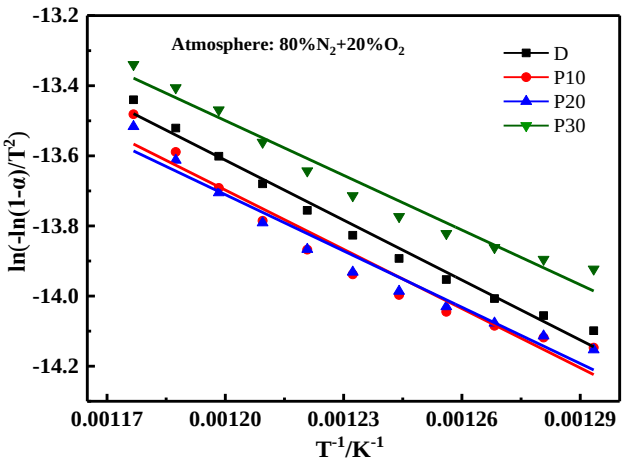


**Fig. 9.** Fitting curves of particle pyrolysis characteristic with Coats-Redfern method.

**Table 4** Calculated kinetic parameters of soot particles.

| Particle sample | Fitting equations | Regression coefficient / $R^2$ | Activation energy E / (kJ/mol) | Pre-exponential factor A / ($min^{-1}$) |
|---|---|---|---|---|
| D | y=-5 698.65x-6.77 | 0.9833 | 47.37 | 130.28 |
| P10 | y=-5 636.16x-6.93 | 0.9501 | 46.85 | 109.78 |
| P20 | y=-5 352.90x-7.28 | 0.9574 | 44.50 | 73.25 |
| P30 | y=-5 201.29x-7.35 | 0.9635 | 43.24 | 66.31 |

### 3.4. Particle microscopic morphology

Fig. 10 gives the microscopic morphology of particle samples with diesel, P10, P20 and P30 fuels under rated condition characterized by means of SEM and magnified 100,000 times. It can be seen from the Fig. 10 that the particles morphology of the blends is similar to that of pure diesel, and the particle size of individual particle is in the range of 30~50nm. Due to the high surface activity of fine particles, the agglomeration is easy to occur between particles, and most of them are chain like or flocculent structure. However, the difference between the blends and diesel fuel is that the particles size changes inconsistently, also the single particle size decreases and the agglomeration degree between particles increases with an increase in PODE blending ratio.

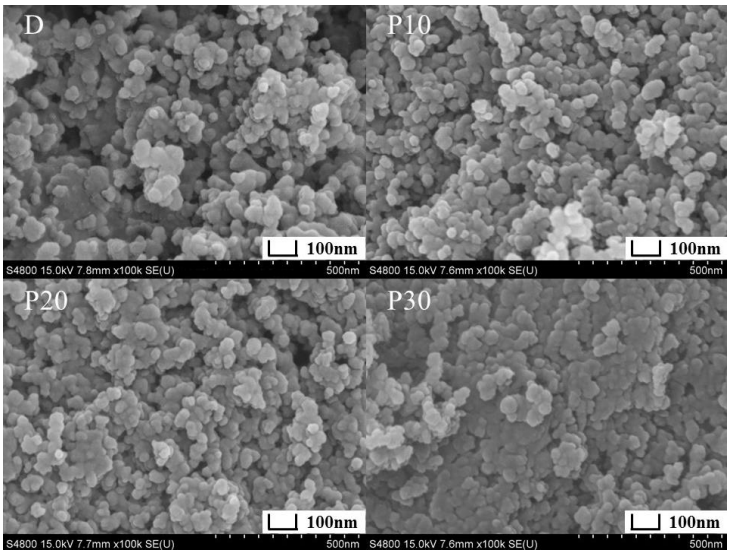


**Fig. 10.** SEM images of particle samples with the blends.

The SEM image of diesel exhaust particles has a typical fractal structure, and the growth mechanism of particles determines its fractal structure characteristics. The agglomeration form of particles is mainly divided into sedimentation under gravity, and the particle diffusion and Brownian motion in the turbulent process. The fractal dimension can be used to quantitatively study the density of the particle geometric structure. The larger the fractal dimension is, the higher the degree of overlap between the base carbon particles is, and the more compact the particle structure is [52]. The self-similar fractal dimension, the box-counting dimension, is applied to investigate the fractal characteristics of PODE/diesel blended fuel

particles in this study. The equation for calculating box-counting dimension is as follows:

$$D_B = -\lim_{r \to 0} \frac{\lg N(r)}{\lg r} \tag{3}$$

where $D_B$ denotes the box-counting dimension of the particle SEM image; $r$ denotes the side length of the square box; $N(r)$ denotes the number of square boxes that completely cover the particle pattern area.

The box-counting dimension of PODE/diesel particles was calculated by MATLAB software as follows: firstly, the image processing is to read the original SEM image of particles; secondly, gray matrix of the image is calculated; thirdly, the threshold of image binarization is calculated; fourth, the fitting equation (4) is obtained by fitting the binary graph covered by a square box with side length $r$. The slope of the fitting equation $D_B$ is the fractal dimension.

$$y = -D_B x + b \tag{4}$$

The binarization threshold of the SEM image and the relationship of $\lg N(r)$-$\lg r$ of diesel particles are obtained via calculating the box-counting dimension of the SEM image of pure diesel combustion particles. The result of fitting the curve is shown in Fig. 11. It can be observed that the regression coefficient of the fitted curve $R^2$ is 0.9959, and the box-counting dimension of diesel particles is 1.913. The box-counting dimensions of P10, P20 and P30 fuel combustion particles can be calculated with the same method. The fitting equations, regression coefficients and box-counting dimensions of the particles with different PODE blending ratios are listed in Table 5. The results show that the $\lg N(r)$-$\lg r$ relationship of P10, P20 and P30 particles are well fitted, and their box-counting dimensions are 1.936, 1.944 and 1.978, respectively. It can be seen that the box-counting dimension of the particles gradually increases with PODE blending ratio, which indicates that the degree of cluster between particles is gradually enhanced.

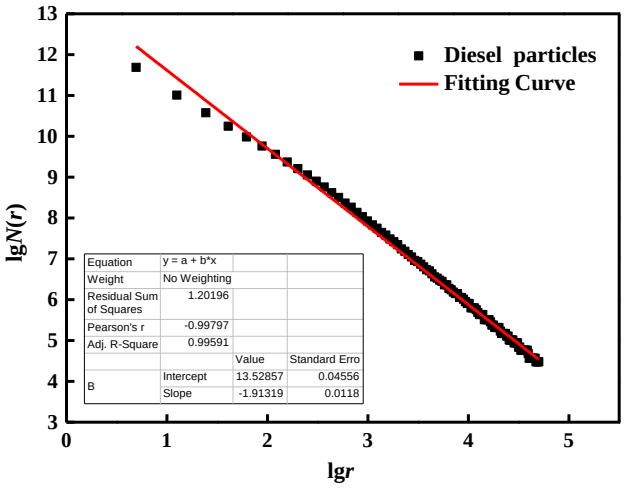


**Fig. 11.** The fitting curve of combustion particles with pure diesel.

**Table 5** Box-counting dimension of PODE/diesel blends particles.

| Particle sample | Fitting equations | Regression coefficient / $R^2$ | $D_B$ |
|---|---|---|---|
| D | y=-1.913x+13.529 | 0.9959 | 1.913 |
| P10 | y=-1.936x+13.624 | 0.9970 | 1.936 |
| P20 | y=-1.944x+13.650 | 0.9970 | 1.944 |
| P30 | y=-1.978x+13.796 | 0.9983 | 1.978 |

## 4. Conclusions

In current study, the particle size distribution and oxidation characteristics of exhaust PM were carried out on a common-rail engine with PODE/diesel blends at various PODE blending ratios by means of EEPS and TGA. The main conclusions are summarized as follows:

(1) PODE/diesel blends can effectively reduce the smoke emission for diesel engines and its decreasing range becomes larger with PODE blending ratio increasing. At rated condition, the smoke emissions of P10, P20 and P30 decrease by 29.7%, 67.8% and 82.4% respectively as compared to pure diesel.

(2) The addition of PODE in diesel fuel can significantly decrease the total particle number, especially at high load. Compared with pure diesel, the total particle number concentrations of P10, P20 and P30 at rated condition are reduced by 15.5%, 27.0% and 28.1%, respectively.

(3) As PODE blending ratio increases, the particle concentration distribution moves towards the direction of small particle size, the proportion of nucleation-mode particles increases, and the proportion of accumulation-mode particles decreases. Also, the peak values of particle number concentration, surface area

concentration and volume concentration decrease, and the particle size at the peak position decrease.

(4) With the increment in PODE blending ratio, the SOF content in exhaust particles increases, the weight loss rates of soot particles and SOF component are increased, and the corresponding peak temperatures are decreased. Meantime, the activation energy of particle pyrolysis is reduced, which indicates that particle oxidation reaction becomes easier with adding PODE to diesel fuel.

(5) Particle microscopic morphology of the blends is similar to that of pure diesel, and the single particle size is in the range of 30~50nm. The morphology of particles sample is mostly chain like or flocculent, and the agglomeration degree between particles increases with the addition of PODE in diesel fuel.

## Acknowledgement

This work was supported by the National Natural Science Foundation of China (No. 51806086) and project funded by China Postdoctoral Science Foundation (No. 2020M672133).

## References

[1] M. Hajbabaei, G. Karavalakis, K.C. Johnson, J. Guthrie, A. Mitchell, T.D. Durbin, Impacts of biodiesel feedstock and additives on criteria emissions from a heavy-duty engine, Fuel Process. Technol. 126 (2014) 402-414.

[2] G. Thomas, B. Feng, A. Veeraragavan, M.J. Cleary, N. Drinnan, Emissions from DME combustion in diesel engines and their implications on meeting future emission norms: A review, Fuel Process. Technol. 119 (2014) 286-304.

[3] J. Fang, Z. Meng, J. Li, Y. Du, Y. Qin, Y. Jiang, W. Bai, G.G. Chase, The effect of operating parameters on regeneration characteristics and particulate emission characteristics of diesel particulate filters, Appl. Therm. Eng. 148 (2019) 860-867.

[4] H. Chen, J. He, H. Hua, Investigation on combustion and emission performance of a common rail diesel engine fueled with diesel/biodiesel/polyoxymethylene dimethyl ethers blends, Energy Fuel 31 (2017) 11710-11722.

[5] H. Huang, C. Zhou, Q. Liu, Q. Wang, X. Wang, An experimental study on the combustion and emission characteristics of a diesel engine under low temperature combustion of diesel/gasoline/n-butanol blends, Appl. Energy 170 (2016) 219-231.

[6] J. Schneider, N. Hock, S. Weimer, S. Borrmann, Nucleation particles in diesel exhaust: Composition inferred from in situ mass spectrometric analysis, Environ. Sci. Technol. 39 (2005) 6153-6161.

[7] P. Zhang, J. He, H. Chen, X. Zhao, L. Geng, Improved combustion and emission characteristics of ethylene glycol/diesel dual-fuel engine by port injection timing and direct injection timing, Fuel Process. Technol. 199 (2020) 106394.

[8] Y. Li, Y. Chen, G. Wu, A new skeletal mechanism for diesel-n-butanol blends combustion in engine, Fuel 264 (2020) 116856.

[9] J. Liu, J. Yang, P. Sun, W. Gao, C. Yang, J. Fang, Compound combustion and pollutant emissions characteristics of a common-rail engine with ethanol homogeneous charge and polyoxymethylene dimethyl ethers injection, Appl. Energy 239 (2019) 1154-1162.

[10] S. Wu, D. Kang, Y. Liu, Z. Wang, R. Xiao, A.L. Boehman, The oxidation of $C_2$-$C_4$ diols and diol/TPGME blends in a motored engine, Fuel 257 (2019) 116093.

[11] J. Liu, L. Feng, H. Wang, Z. Zheng, B. Chen, D. Zhang, M. Yao, Spray characteristics of gasoline/PODE and diesel/PODE blends in a constant volume chamber, Appl. Therm. Eng. 159 (2019) 113850.

[12] L. Tong, H. Wang, Z. Zheng, R. Reitz, M. Yao, Experimental study of RCCI combustion and load extension in a compression ignition engine fueled with gasoline and PODE, Fuel 181 (2016) 878-886.

[13] H. Liu, Z. Wang, Y. Li, Y. Zheng, T. He, J. Wang, Recent progress in the application in compression ignition engines and the synthesis technologies of polyoxymethylene dimethyl ethers, Appl. Energy 233 (2019) 599-611.

[14] N. O'Connell, A. Röll, R. Lechner, T. Luo, M. Brautsch, PODE-blend as pilot fuel in a biomethane dual fuel engine: Experimental analysis of performance, combustion and emissions characteristics, Renew. Energy 143 (2019) 101-111.

[15] M. Härtl, P. Seidenspinner, E. Jacob, G. Wachtmeister, Oxygenate screening on a heavy-duty diesel engine and emission characteristics of highly oxygenated oxymethylene ether fuel $OME_1$, Fuel 153 (2015) 328-335.

[16] Y. Zheng, Q. Tang, T. Wang, Y. Liao, J. Wang, Synthesis of a green diesel fuel additive over cation resins, Chem. Eng. Technol. 36 (2013) 1951-1956.

[17] L. Pellegrini, R. Patrini, M. Marchionna, Effect of POMDME blend on PAH emissions and particulate size distribution from

452 an in-use light-duty diesel engine, In: SAE 2014 world congress: April 8-10, 2014, Detroit, Michigan, USA, Detroit, 2014, pp.
453 13835-13850.
454 [18] J. Liu, H. Wang, Y. Li, Z. Zheng, Z. Xue, H. Shang, M. Yao, Effects of diesel/PODE (polyoxymethylene dimethyl ethers)
455 blends on combustion and emission characteristics in a heavy duty diesel engine, Fuel 177 (2016) 206-216.
456 [19] H. Huang, Q. Liu, W. Teng, M. Pan, C. Liu, Q. Wang, Improvement of combustion performance and emissions in diesel
457 engines by fueling n-butanol/diesel/$PODE_{3-4}$ mixtures, Appl. Energy 227 (2018) 38-48.
458 [20] C. He, J. Li, Y. Wang, J. Tan, G. Song, D. Jia, L. Zhao, Size-segregated particulate matter emission characteristics of a
459 heavy-duty diesel engine with oxygenated fuels, Appl. Therm. Eng. 125 (2017) 1173-1180.
460 [21] C. Barro, M. Parravicini, K. Boulouchos, A. Liati, Neat polyoxymethylene dimethyl ether in a diesel engine; part 2: Exhaust
461 emission analysis, Fuel 234 (2018) 1414-1421.
462 [22] H. Liu, Z. Wang, J. Wang, X. He, Y. Zheng, Q. Tang, J. Wang, Performance, combustion and emission characteristics of a
463 diesel engine fueled with polyoxymethylene dimethyl ethers ($PODE_{3-4}$)/diesel blends, Energy 88 (2015) 793-800.
464 [23] H. Song, C. Liu, F. Li, Z. Wang, X. He, S. Shuai, J. Wang, A comparative study of using diesel and PODEn as pilot fuels for
465 natural gas dual-fuel combustion, Fuel 188 (2017) 418-426.
466 [24] S.W. Kruczyński, Performance and emission of CI engine fuelled with camelina sativa oil, Energy Convers. Manage. 65
467 (2013) 1-6.
468 [25] A.K. Agarwal, A. Dhar, D.K. Srivastava, R.K. Maurya, A.P. Singh, Effect of fuel injection pressure on diesel particulate size
469 and number distribution in a CRDI single cylinder research engine, Fuel 107 (2013) 84-89.
470 [26] L. Qu, Z. Wang, J. Zhang, Influence of waste cooking oil biodiesel on oxidation reactivity and nanostructure of particulate
471 matter from diesel engine, Fuel 181 (2016) 389-395.
472 [27] I. Kang, J. Bae, G. Bae, Performance comparison of autothermal reforming for liquid hydrocarbons, gasoline and diesel for
473 fuel cell applications, J. Power Sources 163 (2006) 538-546.
474 [28] H. Liu, Z. Wang, J. Wang, X. He, Y. Zheng, Q. Tang, J. Wang, Performance, combustion and emission characteristics of a

diesel engine fueled with polyoxymethylene dimethyl ethers (PODE3-4)/ diesel blends, Energy 88 (2015) 793-800.

[29] J. Liu, P. Sun, H. Huang, J. Meng, X. Yao, Experimental investigation on performance, combustion and emission characteristics of a common-rail diesel engine fueled with polyoxymethylene dimethyl ethers-diesel blends, Appl. Energy 202 (2017) 527-536.

[30] A. Datta, B.K. Mandal, Impact of alcohol addition to diesel on the performance combustion and emissions of a compression ignition engine, Appl. Therm. Eng. 98 (2016) 670-682.

[31] M. Lapuerta, J. Rodríguez–Fernández, J. Sánchez-Valdepeñas, Soot reactivity analysis and implications on diesel filter regeneration, Process. Energy Combust. Sci. 78 (2020) 100833.

[32] D. Li, Y. Gao, S. Liu, Z. Ma, Y. Wei, Effect of polyoxymethylene dimethyl ethers addition on spray and atomization characteristics using a common rail diesel injection system, Fuel 186 (2016) 235-247.

[33] G. Li, J. Cao, M. Li, Y. Quan, Z. Chen, Experimental study on the size distribution characteristics of spray droplets of DME/diesel blended fuels, Fuel Process. Technol. 104 (2012) 352-355.

[34] B. Jiang, D. Liu, Z. Lin, Soot particles diagnostics in ethylene inverse diffusion flame blending with biodiesel surrogates of saturated methyl butyrate and unsaturated methyl crotonate, Fuel Process. Technol. 202 (2020) 106379.

[35] F.G. Cuenca, M.G. Marín, M.B.F. Díaz, The influence of propylene glycol ethers on base diesel properties and emissions from a diesel engine, Energy Convers. Manage. 75 (2013) 741-747.

[36] H. Chu, L. Xiang, X. Nie, Y. Ya, M. Gu, J. E, Laminar burning velocity and pollutant emissions of the gasoline components and its surrogate fuels: A review, Fuel, 269 (2020) 11745.

[37] Y.R. Tan, M.L. Botero, Y. Sheng, J.A.H. Dreyer, R. Xu, W. Yang, M. Kraft, Sooting characteristics of polyoxymethylene dimethyl ether blends with diesel in a diffusion flame, Fuel 224 (2018) 499-506.

[38] T. Chu Van, Z. Ristovski, N. Surawski, T.A. Bodisco, S.M.A. Rahman, J. Alroe, B. Miljevic, F.M. Hossain, K. Suara, T. Rainey, R.J. Brown, Effect of sulphur and vanadium spiked fuels on particle characteristics and engine performance of auxiliary diesel engines, Environ. Pollut. 243 (2018) 1943-1951.

[39] T. Lu, Z. Huang, C.S. Cheung, J. Ma, Size distribution of EC, OC and particle-phase PAHs emissions from a diesel engine fueled with three fuels, Sci. Total Environ. 438 (2012) 33-41.

[40] U. Kirchner, V. Scheer, R. Vogt, R. Kägi, TEM study on volatility and potential presence of solid cores in nucleation mode particles from diesel powered passenger cars, J. Aerosol Sci. 40 (2009) 55-64.

[41] W. Zhang, X. Chen, G. Gu, H. Hu, T. Liu, Z. Huang, Experimental study of the spray characteristics of USLD, methanol and DME on the swirl nozzle of a Stirling engine, Fuel Process. Technol. 119 (2014) 1-9.

[42] S. Wu, D. Kang, H. Zhang, R. Xiao, A.L. Boehman, The oxidation characteristics of furan derivatives and binary TPGME blends under engine relevant conditions, Proc. Combus. Inst. 37 (2019) 4635-4643.

[43] H. Chen, R. Huang, H. Huang, M. Pan, W. Teng, Potential improvement in particulate matter's emissions reduction from diesel engine by addition of PODE and injection parameters, Appl. Therm. Eng.150 (2019) 591-604.

[44] H. Chen, X. Su, J.H. Li, X.L. Zhong, Effects of gasoline and polyoxymethylene dimethyl ethers blending in diesel on the combustion and emission of a common rail diesel engine, Energy 171 (2019) 981-999.

[45] J. Benajes, A. García, J.M. Serrano, V. Boronat, Gaseous emissions and particle size distribution of dual-mode dual-fuel diesel-gasoline concept from low to full load, Appl. Therm. Eng. 120 (2017) 138-149.

[46] Z. Dou, C. Yao, H. Wei, B. Wang, M. Liu, C. Chen, J. Gao, J. Shi, Experimental study of the effect of engine parameters on ultrafine particle in diesel/methanol dual fuel engine, Fuel 192 (2017) 45-52.

[47] C. Yao, Z. Dou, B. Wang, M. Liu, H. Lu, J. Feng, L. Feng, Experimental study of the effect of heavy aromatics on the characteristics of combustion and ultrafine particle in DISI engine, Fuel 203 (2017) 290-297.

[48] W. Gao, J. Liu, P. Sun, C. Yang, J. Fang, Gaseous emissions and particle microstructure characteristics of PODE/diesel blend fuel, Int. J. Automot. Technol. 20 (2019) 607-617.

[49] Z. Zhang, R. Balasubramanian, Effects of oxygenated fuel blends on the composition of size-segregated engine-out diesel particulate emissions and on the toxicity of quasi-ultrafine particles, Fuel 215 (2018) 161-170.

[50] J. Liu, J. Yang, P. Sun, Q. Ji, J. Meng, P. Wang, Experimental investigation of in-cylinder soot distribution and exhaust

particle oxidation characteristics of a diesel engine with nano-$CeO_2$ catalytic fuel, Energy 161 (2018) 17-27.

[51] J. Liu, L. Wang, P. Sun, P. Wang, Y. Li, H. Ma, P. Wu, Z. Liu, Effects of iron-based fuel borne catalyst addition on microstructure, element composition and oxidation activity of diesel exhaust particles, Fuel 270 (2020) 117597.

[52] M. Altenhoff, S. Aßmann, C. Teige, F.J.T. Huber, S. Will, An optimized evaluation strategy for a comprehensive morphological soot nanoparticle aggregate characterization by electron microscopy, J. Aerosol Sci. 139 (2020) 105470.